

Published in final edited form as:

FEBS Lett. 2013 November 1; 587(21): . doi:10.1016/j.febslet.2013.09.006.

Blockade of Islet Amyloid Polypeptide Fibrillation and Cytotoxicity by the Secretory Chaperones 7B2 and proSAAS

Juan R. Peinado^{1,#}, Furqan Sami¹, Nina Rajpurohit¹, and Iris Lindberg^{1,*}

¹Department of Anatomy and Neurobiology, University of Maryland-Baltimore, Baltimore, MD 21201

Abstract

The deposition of fibrillated human islet β -cell peptide islet amyloid polypeptide (hIAPP) into amyloid plaques is characteristic of the pathogenesis of islet cell death during type 2 diabetes. We investigated the effects of the neuroendocrine secretory proteins 7B2 and proSAAS on hIAPP fibrillation in vitro and on cytotoxicity. In vitro, 21-kDa 7B2 and proSAAS blocked hIAPP fibrillation. Structure-function studies showed that a central region within 21-kDa 7B2 is important in this effect and revealed the importance of the N-terminal region of proSAAS. Both chaperones blocked the cytotoxic effects of exogenous hIAPP on Rin5f cells; 7B2 generated by overexpression was also effective. ProSAAS and 7B2 may perform a chaperone role as secretory anti-aggregants in normal islet cell function and in type 2 diabetes.

Keywords

type 2 Diabetes; hIAPP; 7B2; proSAAS

Introduction

Amyloid formation plays a critical role in many different human diseases, including Huntington's disease (HD), Parkinson's disease (PD), Alzheimer's disease (AD) and type 2 diabetes mellitus (T2DM). Among these diseases, T2DM together with AD are leading causes of morbidity and mortality in the elderly. Both diseases share common clinical and biochemical features [1], including functional tissue loss due to accumulation and aggregation of small peptides, such as islet amyloid polypeptide in the pancreas of T2DM patients, or beta amyloid in AD patients. Specifically, islet amyloid polypeptide (IAPP) fibrils arise following initial increased production of IAPP which leads to oligomeric aggregation of IAPP molecules that then assemble into amyloid fibrils in pancreatic islets, eventually resulting in pancreatic beta cell loss [2-4]. Beta cell dysfunction leads to progressive impairment of insulin secretion and ultimately to overt T2DM [2]. Interestingly, only human IAPP (hIAPP), but not rodent IAPP, forms oligomers and fibrils [5], and expression of hIAPP in rats causes formation of islet amyloid plaques, loss of β -cells, and consequent diabetes [6].

© 2013 Federation of European Biochemical Societies. Published by Elsevier B.V. All rights reserved.

*To whom correspondence should be addressed: Iris Lindberg, Department of Anatomy and Neurobiology University of Maryland-Baltimore 20 Penn Street, HSF2, RmS251, Baltimore, MD 21201 Phone: 410-706-4778 ilind001@umaryland.edu.

#Present address: Dept. of Medical Sciences, University of Castilla-La Mancha, 13071 Ciudad Real, Spain.

Publisher's Disclaimer: This is a PDF file of an unedited manuscript that has been accepted for publication. As a service to our customers we are providing this early version of the manuscript. The manuscript will undergo copyediting, typesetting, and review of the resulting proof before it is published in its final citable form. Please note that during the production process errors may be discovered which could affect the content, and all legal disclaimers that apply to the journal pertain.

IAAP is co-secreted with insulin from pancreatic β -cells [7]. Both IAPP and insulin are synthesized from larger precursors after being proteolytically cleaved by PC1/3 and PC2 (prohormone convertases 1/3 and 2) and carboxypeptidase E [8]. Both PC1/3 and PC2 have been shown to interact with specific binding proteins, proSAAS and 7B2 respectively; these proteins modulate convertase traffic through the secretory pathway, and, in the case of 7B2, perform an important anti-aggregant function [9-11]. Abundant expression of both convertases [12-14] and chaperones [15, 16] has been demonstrated in islet cells and studied in the context of diabetes and function in glucagon and insulin synthesis. As the tissue distributions of 7B2 and proSAAS are much broader than those of the convertases [17], additional functions are currently being investigated. The recent discovery of 7B2 as a potent inhibitor of beta amyloid and synuclein aggregation supports the idea that this family of chaperones may serve as general secretory chaperones, acting to prevent aggregation of proteins in AD and PD [18] and possibly in other diseases which involve amyloid formation.

To investigate the potential inhibitory effect of 7B2 and proSAAS in preventing hIAPP fibrillation, we have carried out an *in vitro* fluorescence-based fibrillation study. We have also evaluated the effect of both chaperones added extracellularly, in reducing the cytotoxicity of hIAPP in Rin5f insulinoma cells. Lastly, we have tested the potential effect of intracellularly-expressed 7B2 and proSAAS.

Materials and Methods

Materials

Human IAPP (hIAPP) was purchased from Bachem and resuspended in DMSO at a concentration of 1 mM; 20 μ l aliquots were stored at -80 C and resuspended in 20 mM Tris-HCl, pH 7.5, to a working concentration of 100 μ M just before use.

Preparation of His-tagged 21-kDa 7B2 and 21 kDa proSAAS and truncated proteins

Recombinant His-tagged 21-kDa 7B2 and 7B2 polypeptides 30–150 and 68–150 were prepared using the QIAexpress system (Qiagen). Primers were designed as described previously [19]. PCR fragments were cloned into pQE30, and sequences were verified by DNA sequencing. Proteins were expressed in *Escherichia coli* XL1-Blue (Stratagene) and purified with the guanidine HCl/ refolding method as described previously [20]. Briefly, bacterial overexpression was accomplished by IPTG induction and overnight incubation of cultures at 26 C. Proteins were isolated via His-tag chromatography and dialysis against phosphate-buffered saline.

21-kDa mouse His-tagged proSAAS (proSAAS 1-180) protein was prepared as described previously [21]. ProSAAS¹³⁸⁻¹⁸⁰ and proSAAS⁹⁷⁻¹³⁷ were synthesized at more than 85% purity at the University of Maryland-Baltimore, Biopolymer Core Facility.

In vitro fibrillation assays

hIAPP (10 μ M final concentration) was fibrillated in 96-well white Nunc polycarbonate plates [22] in 20 mM Tris-HCl buffer, pH 7.4, in the presence or absence of either the 21-kDa 7B1 and proSAAS proteins or N-terminally truncated fragments at the final concentrations indicated in the figures; carbonic anhydrase (CA) and insulin were used as negative and positive controls respectively. The reaction was carried out in triplicate in a total volume of 100 μ l at 25 C, and the final concentration of ThT was 20 μ M; a Molecular Devices spectrofluorometer was used. Fibrillation was measured as an increase in ThT fluorescence (excitation wavelength 444 nm, emission 485 nm; [23]) upon binding to fibrils. The data were then normalized: the lowest ThT fluorescence value detected was set at 0% (time 0) and the highest ThT fluorescence value for the assay was set at 100%.

Cell culture and cytotoxicity assays

Rat insulinoma (Rin5f) cells were maintained in high glucose DMEM and neuroblastoma (Neuro2A) cells in 50% DMEM and 50% Optimem. Both media were supplemented with 10% fetal bovine serum (FBS; Atlanta Biologicals) and the cells cultured at 37 C in a humidified atmosphere containing 5% CO₂. For cytotoxicity assays Rin5f cells were plated in 96-well plates at a density of about 50%. On the following day, cells were washed with serum-free medium and treated with either vehicle, 21-kDa 7B2 (15 μM), 21-kDa proSAAS (15 μM), or carbonic anhydrase (5 μM) as a negative control, for 48 h. Cell viability was measured using the WST-1 cell proliferation reagent (Roche, Mannheim) and absorbance at 450 nm was measured every 30 min. The value for vehicle-treated cells was set as 100%. Neuro2A cells were transiently transfected with vectors encoding rat 21-kDa 7B2 and mouse 27-kDa proSAAS for 24h in a 96 well plate using the FuGENE-HD transfection reagent (Promega) as suggested by the manufacturer. Cells were incubated for an additional 24 h in serum-free media with 5 μM hIAPP before measuring cellular survival rates. In one experiment, media and cells were collected for verification of chaperone expression in media and cells by Western blotting.

Bioinformatics and statistical analysis

Prediction of α-helices in proSAAS was performed using the GORIV and CFSSP programs through the ExPasy server (expasy.org) and also with PSIPRED (bioinf.cs.ucl.ac.uk). A tentative 3D proSAAS model was made using BIOSERF based on the best-scoring hits using PSI-BLAST, pGenTHREADER and HHPred at UCL-CS Bioinformatics [24]. Potential disorder in proSAAS was investigated using DISOPRED at UCL-CS Bioinformatics, and coiled-coils identified by MARCOIL at the ExPasy server. For statistical analysis, either the Student's unpaired t-test, or a one-way ANOVA followed by Newman-Keuls multiple comparison was used to assess significance, as indicated in each figure; p-values with a value of p<0.05 were taken as statistically significant.

Results

In vitro fibrillation assay

We investigated hIAPP fibrillation using an *in vitro* fluorescence assay using a ThT assay. In our hands, concentrations ranging from 5 to 20 μM of hIAPP exhibited complete fibrillation within an hour at 25 C and 10 μM was chosen for further assays (**Fig. 1A**). It has been shown that fibrillation of hIAPP is inhibited by insulin [25]. In our assays 5 μM insulin blocked 80% of hIAPP fibrillation, while an irrelevant control protein such as carbonic anhydrase did not block fibrillation (**Fig. 1B**). We also found that fibrillation of hIAPP was accelerated in the presence of salts, while detergents such as Triton X-100 inhibited the reaction (data not shown); therefore, the fibrillation assays were carried out in a minimal salt-containing, detergent-free buffer.

21-kDa 7B2 and proSAAS block hIAPP fibrillation in vitro

Previous work in our laboratory has shown that the secretory chaperone 7B2 not only colocalizes with amyloid plaques but also inhibits beta amyloid fibrillation [18]. Since 7B2 is abundant in the pancreas [26] we investigated the possibility that 7B2 may also inhibit hIAPP fibrillation. We found 90% inhibition of hIAPP fibrillation with 10 μM 7B2, while 1 μM resulted in 50% inhibition (**Fig. 1C**). ProSAAS is also abundant in the pancreas [27]; in order to evaluate whether proSAAS also possesses anti-fibrillation ability, we carried out an assay using proSAAS concentrations between 0.1 and 10 μM. Under these conditions 10 μM 21 kDa proSAAS blocked hIAPP fibrillation completely and 0.1 μM still retained some inhibitory activity on fibril formation (**Fig. 1D**).

Residues 30-180 of 21-kDa 7B2 are sufficient to block fibrillation of hIAPP

To elucidate the region within 7B2 responsible for the anti-fibrillation effect, we performed *in vitro* fibrillation assays with N-terminally truncated proteins. Structure-function analysis using truncated forms of 7B2 revealed that the anti-aggregation effect was greatest using 21-kDa 7B2 (**Fig. 2A**), although 10 μ M 7B2³⁰⁻¹⁵⁰ and 7B2⁶⁸⁻¹⁵⁰ partially inhibited hIAPP fibrillation by 30 and 20% respectively (**Fig. 2B**).

The N-terminal region of proSAAS is important for inhibition of hIAPP fibrillation

Bioinformatics research on the secondary structure of proSAAS was performed as an attempt to identify potential structures related to its function as anti-aggregant. Various bioinformatics approaches (see *Materials and Methods*) led us to identify 3 major regions with alpha helical character, which lie between the disordered regions predicted for proSAAS (**Supplemental Figure 1A**). Interestingly, these bioinformatics predictions identified a coiled-coil region with higher than 93% probability scores (amino acids³⁴⁻⁷⁹; **Supplemental Figures 1B and C**). The location of these identified alpha helices in the 3D structure was performed by homology prediction, as indicated in the *Materials and Methods* (**Supplemental Figure 1D**). According to this prediction, two truncated peptides (**Fig. 3A**) were synthesized (proSAAS⁹⁷⁻¹³⁷ and proSAAS¹³⁸⁻¹⁸⁰, see *Materials and Methods*) to test whether α -helices II and III play a role in proSAAS-induced inhibition of fibrillation. However, neither of these two peptides was able to inhibit fibrillation *in vitro* (**Fig. 3B**). We conclude that residues 1-97 in the N-terminal domain contain key determinants for the anti-fibrillation ability of proSAAS on hIAPP.

21-kDa 7B2 and 21-kDa proSAAS block hIAPP-mediated cytotoxicity

Insoluble hIAPP amyloid aggregates colocalize with β cells, and their formation is linked to the progressive deterioration of β cells (reviewed in [28]). In addition, soluble hIAPP amyloid aggregates have also been suggested to be cytotoxic [29, 30]. Therefore, we treated Rin5f insulinoma cells with recombinant 7B2 and proSAAS to test whether they could exert cytoprotective effects against hIAPP cytotoxicity. We observed that 10 μ M hIAPP, the concentration used for the *in vitro* fibrillation assays, resulted in less than 20% cell death, while 20 μ M and higher doses resulted in complete cell death (data not shown). We therefore chose a concentration of 15 μ M hIAPP for our cytotoxicity assays, which resulted in approximately 75% cell death (**Fig. 4**). Both 7B2 and proSAAS, at equimolar concentrations to hIAPP, protected the cells from hIAPP-mediated cytotoxicity. Incubation of the cells with both chaperones resulted in less than 20% cell death, which is comparable with the results obtained with insulin (**Fig. 4**). To investigate whether toxicity was due to fibrillated or unfibrillated hIAPP we conducted an *in vitro* fibrillation assay that mimicked the conditions of the toxicity assay. We found that in the presence of Rin5f culture media only a small percentage of the hIAPP was fibrillated after 24 h (**Supplemental Figure 2A**), suggesting that fibrils are not the cause of hIAPP cytotoxicity.

Transfection of 7B2 cDNA into Neuro2A cells partially protects cells from hIAPP toxicity

In order to evaluate the ability of intracellularly-expressed 7B2 and proSAAS to protect from hIAPP toxicity, we used neuroblastoma cells (Neuro2A), which express lower levels of endogenous 7B2 and a much higher transfection efficiency. Initial experiments indicated that concentrations of hIAPP as low as 5 μ M resulted in strong cytotoxicity effect in this cell line (**Fig. 5A and B**). Transient transfection of 7B2 cDNA, in which expression was confirmed by Western blotting of cell extracts and media (**Supplemental Fig. 2B**), resulted in a significant increase in cell proliferation when compared to cells transfected with empty vector; similar effects were not obtained using proSAAS cDNA. Interestingly, when the 7B2-transfected cells were examined under the microscope, they did not show signs of

apoptosis (**Fig. 5A**), indicating that although the 7B2-transfected cells did not proliferate similarly to the untreated cells, they were still viable.

Discussion

Increasing evidence indicates that the small proprotein convertase binding proteins proSAAS and 7B2 are involved in chaperone functions in neuroendocrine tissues. In addition to its role in blocking proPC2 aggregation [11, 31], 7B2 also displays anti-aggregant properties against neurodegeneration-related proteins such as β -amyloid and α -synuclein [18]. Similar effects have been shown for 7B2 in blocking the aggregation of insulin-like growth factor 1 (IGF1; [32]). Herein, we have demonstrated that added 7B2 can block both *in vitro* fibrillation of hIAPP and the cytotoxic effects of hIAPP on Rin5f cells. The inhibition by 7B2 and its N-terminally truncated proteins on hIAPP fibrillation resembles the results observed for inhibition of beta amyloid fibrillation [18]; therefore, we propose that 7B2 interferes with both A β 1-42 and hIAPP oligomerization via a similar molecular basis. This idea is also supported by results showing a reduction in hIAPP cytotoxicity after 7B2 addition. It has been proposed that AD and non-insulin-dependent T2DM may share a common mechanism of cell death which is related to the toxicity of beta amyloid and hIAPP oligomers, respectively [33, 34]. Type 2 diabetes constitutes a chronic metabolic disorder that increases the risk for cerebrovascular disease and for dementia [35, 36]. Interestingly, although there is no evidence of hIAPP synthesis in the brain, the presence of hIAPP oligomers and plaques in the temporal lobe gray matter from diabetic patients has been recently identified [37]. 7B2 is abundant in both brain and pancreatic islets, where it is likely co-secreted from neurons together with beta amyloid and from beta cells together with hIAPP, respectively. The inhibitory effect of 7B2 on hIAPP aggregation supports the idea that 7B2 may represent a defensive mechanism against hIAPP deposition *in vivo* in type-2 derived amyloid pathologies.

Since fibrils do not form efficiently in Neuro2A cell medium, 7B2 may protect cells from hIAPP toxicity by blocking toxic oligomer formation rather than by blocking fibrillation. Alternatively, or in addition, 7B2 may interfere with the interaction of hIAPP with its receptor, thought to consist of a complex of the calcitonin receptor coupled to a receptor modifying protein (reviewed in [38]). The mechanism of chaperone cytoprotection deserves further exploration.

In human diabetic pancreas of individuals suffering with β -cell dysfunction and development of T2DM, hIAPP amyloid aggregates are found exclusively extracellularly around islets (reviewed in [28]), although studies on nude mice with transplanted human islets [39] and in transgenic mice expressing hIAPP [40] have indicated that the early stages of islet amyloid formation may take place intracellularly. However, in our experiments, the primary effect of 7B2 in blocking cytotoxicity is likely to occur extracellularly, as the majority of endogenous 7B2 is secreted by Neuro2A cells.

ProSAAS, a small neuroendocrine protein with structural resemblance to 7B2, also interacts with a convertase, PC1/3 [25], and overexpression of this protein reduces its secretion [21]. Recent findings indicate that proSAAS has a much broader distribution pattern with respect to PC1/3 in the brain, and its abundance within the pancreas has also been shown [16]. Furthermore, it has recently been shown to constitute one of the most abundant proteins within mature secretory granules in INS1-E insulinoma cells [41]. These findings led us to hypothesize that proSAAS may also perform additional functions in the pancreas. Herein, we have demonstrated that proSAAS suppresses the fibrillation of hIAPP proteins *in vitro* while also protecting insulinoma cells from hIAPP cytotoxicity when added extracellularly. Our structural analysis of proSAAS revealed that the region between residues 35 to 80

constitutes a potential coiled-coil, an idea which is in consonance with homology modeling predictions indicating the possible existence of an alpha helical structure in this region (**Supplemental Fig. 1D**); such a helix is necessary for coiled-coil interactions. We propose that this region may functionally interact with hIAPP, as α -helices II and II alone do not inhibit fibrillation. Interestingly, in contrast to proSAAS, N-terminally truncated forms of 7B2 still retained some inhibitory activity, and did not increase fibrillation.

Previous studies have attempted to identify inhibitors of hIAPP aggregation (*i.e.* resveratrol [42]), as well as endogenous secretory proteins with anti-aggregation activity. The data presented here show that the neuroendocrine chaperone proteins 7B2 and proSAAS, both expressed in beta cells, contain specific molecular features which permit effective inhibition of hIAPP fibrillation *in vitro*, and toxicity *in vivo*. Understanding the molecular mechanisms of hIAPP-chaperone interaction will be an important step toward understanding hIAPP aggregation and cytotoxicity in the development of type 2 diabetes.

Supplementary Material

Refer to Web version on PubMed Central for supplementary material.

Acknowledgments

This work was funded by NIH DK49703 to IL.

Abbreviations

T2DM	Type 2 diabetes
AD	Alzheimer's disease
PD	Parkinson's disease
PC1/3	prohormone convertase 1/3
PBS	phosphate-buffered saline
BSA	bovine serum albumin
TBS	Tris-buffered saline
ThT	Thioflavin T
FBS	fetal bovine serum
IAPP	Islet amyloid polypeptide
CA	carbonic anhydrase

References

1. Gotz J, Itner LM, Lim YA. Common features between diabetes mellitus and Alzheimer's disease. *Cell Mol Life Sci.* 2009; 66:1321–1325. [PubMed: 19266159]
2. Haataja L, Gurlo T, Huang CJ, Butler PC. Islet amyloid in type 2 diabetes, and the toxic oligomer hypothesis. *Endocr Rev.* 2008; 29:303–316. [PubMed: 18314421]
3. Konarkowska B, Aitken JF, Kistler J, Zhang S, Cooper GJ. The aggregation potential of human amylin determines its cytotoxicity towards islet beta-cells. *FEBS J.* 2006; 273:3614–3624. [PubMed: 16884500]
4. Goldsbury C, Goldie K, Pellaud J, Seelig J, Frey P, Muller SA, Kistler J, Cooper GJ, Aebi U. Amyloid fibril formation from full-length and fragments of amylin. *J Struct Biol.* 2000; 130:352–362. [PubMed: 10940238]

5. Janson J, Soeller WC, Roche PC, Nelson RT, Torchia AJ, Kreutter DK, Butler PC. Spontaneous diabetes mellitus in transgenic mice expressing human islet amyloid polypeptide. *Proc Natl Acad Sci U S A*. 1996; 93:7283–7288. [PubMed: 8692984]
6. Butler AE, Jang J, Gurlo T, Carty MD, Soeller WC, Butler PC. Diabetes due to a progressive defect in beta-cell mass in rats transgenic for human islet amyloid polypeptide (HIP Rat): a new model for type 2 diabetes. *Diabetes*. 2004; 53:1509–1516. [PubMed: 15161755]
7. Kahn SE, D'Alessio DA, Schwartz MW, Fujimoto WY, Ensink JW, Taborsky GJ Jr, Porte D Jr. Evidence of cosecretion of islet amyloid polypeptide and insulin by beta-cells. *Diabetes*. 1990; 39:634–638. [PubMed: 2185112]
8. Wang J, Xu J, Finnerty J, Furuta M, Steiner DF, Verchere CB. The prohormone convertase enzyme 2 (PC2) is essential for processing pro-islet amyloid polypeptide at the NH₂-terminal cleavage site. *Diabetes*. 2001; 50:534–539. [PubMed: 11246872]
9. Basak A, Koch P, Dupelle M, Fricker LD, Devi LA, Chretien M, Seidah NG. Inhibitory specificity and potency of proSAAS-derived peptides toward proprotein convertase 1. *J Biol Chem*. 2001; 276:32720–32728. [PubMed: 11435430]
10. Muller L, Lindberg I, Moldave K. The cell biology of the prohormone convertases PC1 and PC2. *Progress in Nucleic Acids Research*. 1999; 63:69–108.
11. Lee SN, Lindberg I. 7B2 prevents unfolding and aggregation of prohormone convertase 2. *Endocrinology*. 2008; 149:4116–4127. [PubMed: 18467442]
12. Malide D, Seidah NG, Chretien M, Bendayan M. Electron microscopic immunocytochemical evidence for the involvement of the convertases PC1 and PC2 in the processing of proinsulin in pancreatic β -cells. *J Histochem Cytochem*. 1995; 43:11–19. [PubMed: 7822759]
13. Wang J, Osei K. Proinsulin maturation disorder is a contributor to the defect of subsequent conversion to insulin in beta-cells. *Biochem Biophys Res Commun*. 2011; 411:150–155. [PubMed: 21723250]
14. Nie Y, Nakashima M, Brubaker PL, Li QL, Perfetti R, Jansen E, Zambre Y, Pipeleers D, Friedman TC. Regulation of pancreatic PC1 and PC2 associated with increased glucagon-like peptide 1 in diabetic rats. *J Clin Invest*. 2000; 105:955–965. [PubMed: 10749575]
15. Portela-Gomes GM, Grimelius L, Stridsberg M. Prohormone convertases 1/3, 2, furin and protein 7B2 (Secretogranin V) in endocrine cells of the human pancreas. *Regul Pept*. 2008; 146:117–124. [PubMed: 17959263]
16. Cras-Meneur C, Inoue H, Zhou Y, Ohsugi M, Bernal-Mizrachi E, Pape D, Clifton SW, Permutt MA. An expression profile of human pancreatic islet mRNAs by Serial Analysis of Gene Expression (SAGE). *Diabetologia*. 2004; 47:284–299. [PubMed: 14722648]
17. Morgan DJ, Mzhavia N, Peng B, Pan H, Devi LA, Pintar JE. Embryonic gene expression and pro-protein processing of proSAAS during rodent development. *J Neurochem*. 2005; 93:1454–1462. [PubMed: 15935061]
18. Helwig M, Hoshino A, Berridge C, Lee SN, Lorenzen N, Otzen DE, Eriksen JL, Lindberg I. The neuroendocrine protein 7B2 suppresses the aggregation of neurodegenerative disease-related proteins. *J Biol Chem*. 2013; 288:1114–1124. [PubMed: 23172224]
19. Muller L, Zhu P, Juliano MA, Juliano L, Lindberg I. A 36-residue peptide contains all of the information required for 7B2-mediated activation of prohormone convertase 2. *J Biol Chem*. 1999; 274:21471–21477. [PubMed: 10409712]
20. Zhu X, Lamango NS, Lindberg I. Involvement of a polyproline helix-like structure in the interaction of 7B2 with prohormone convertase 2. *J Biol Chem*. 1996; 271:23582–23587. [PubMed: 8798569]
21. Fortenberry Y, Hwang JR, Apletalina EV, Lindberg I. Functional characterization of ProSAAS: similarities and differences with 7B2. *J Biol Chem*. 2002; 277:5175–5186. [PubMed: 11719503]
22. Cao P, Meng F, Abedini A, Raleigh DP. The ability of rodent islet amyloid polypeptide to inhibit amyloid formation by human islet amyloid polypeptide has important implications for the mechanism of amyloid formation and the design of inhibitors. *Biochemistry*. 2010; 49:872–881. [PubMed: 20028124]
23. LeVine H 3rd. Quantification of beta-sheet amyloid fibril structures with thioflavin T. *Methods Enzymol*. 1999; 309:274–284. [PubMed: 10507030]

24. Lobley A, Sadowski MI, Jones DT. pGenTHREADER and pDomTHREADER: new methods for improved protein fold recognition and superfamily discrimination. *Bioinformatics*. 2009; 25:1761–1767. [PubMed: 19429599]
25. Westermark P, Li ZC, Westermark GT, Leckstrom A, Steiner DF. Effects of beta cell granule components on human islet amyloid polypeptide fibril formation. *FEBS Lett*. 1996; 379:203–206. [PubMed: 8603689]
26. Mbikay M, Seidah NG, M C. Neuroendocrine secretory protein 7B2: structure, expression and functions. *Biochem J*. 2001; 357:329–342. [PubMed: 11439082]
27. Alarcon C, Verchere CB, Rhodes CJ. Translational control of glucose-induced islet amyloid polypeptide production in pancreatic islets. *Endocrinology*. 2012; 153:2082–2087. [PubMed: 22408171]
28. Hull RL, Westermark GT, Westermark P, Kahn SE. Islet amyloid: a critical entity in the pathogenesis of type 2 diabetes. *J Clin Endocrinol Metab*. 2004; 89:3629–3643. [PubMed: 15292279]
29. Kapurniotu A. Amyloidogenicity and cytotoxicity of islet amyloid polypeptide. *Biopolymers*. 2001; 60:438–459. [PubMed: 12209476]
30. Janson J, Ashley RH, Harrison D, McIntyre S, Butler PC. The mechanism of islet amyloid polypeptide toxicity is membrane disruption by intermediate-sized toxic amyloid particles. *Diabetes*. 1999; 48:491–498. [PubMed: 10078548]
31. Braks JAM, Martens GJM. 7B2 is a neuroendocrine chaperone that transiently interacts with prohormone convertase PC2 in the secretory pathway. *Cell*. 1994; 78:263–273. [PubMed: 7913882]
32. Chaudhuri B, Stephen C, Huijbregts R, Martens G. The neuroendocrine protein 7B2 acts as a molecular chaperone in the in vitro folding of human insulin-like growth factor-1 secreted from yeast. *Biochem Biophys Res Commun*. 1995; 211:417–425. [PubMed: 7794252]
33. Lorenzo A, Yankner BA. Amyloid fibril toxicity in Alzheimer's disease and diabetes. *Ann N Y Acad Sci*. 1996; 777:89–95. [PubMed: 8624132]
34. May PC, Boggs LN, Fuson KS. Neurotoxicity of human amylin in rat primary hippocampal cultures: similarity to Alzheimer's disease amyloid-beta neurotoxicity. *J Neurochem*. 1993; 61:2330–2333. [PubMed: 8245987]
35. Craft S. The role of metabolic disorders in Alzheimer disease and vascular dementia: two roads converged. *Arch Neurol*. 2009; 66:300–305. [PubMed: 19273747]
36. Debette S, Seshadri S, Beiser A, Au R, Himali JJ, Palumbo C, Wolf PA, DeCarli C. Midlife vascular risk factor exposure accelerates structural brain aging and cognitive decline. *Neurology*. 2011; 77:461–468. [PubMed: 21810696]
37. Jackson K, Barisone GA, Diaz E, Jin LW, Decarli C, Despa F. Amylin deposition in the brain: A second amyloid in Alzheimer disease? *Ann Neurol*. 2013 doi: 10.1002/ana.23956.
38. Westermark P, Andersson A, Westermark GT. Islet amyloid polypeptide, islet amyloid, and diabetes mellitus. *Physiol Rev*. 2011; 91:795–826. [PubMed: 21742788]
39. Westermark G, Westermark P, Eizirik DL, Hellerstrom C, Fox N, Steiner DF, Andersson A. Differences in amyloid deposition in islets of transgenic mice expressing human islet amyloid polypeptide versus human islets implanted into nude mice. *Metabolism*. 1999; 48:448–454. [PubMed: 10206436]
40. Westermark GT, Steiner DF, Gebre-Medhin S, Engstrom U, Westermark P. Pro islet amyloid polypeptide (ProIAPP) immunoreactivity in the islets of Langerhans. *Ups J Med Sci*. 2000; 105:97–106. [PubMed: 11095107]
41. Schvartz D, Brunner Y, Coute Y, Foti M, Wollheim CB, Sanchez JC. Improved characterization of the insulin secretory granule proteomes. *J Proteomics*. 2012; 75:4620–4631. [PubMed: 22569486]
42. Mishra R, Sellin D, Radovan D, Gohlke A, Winter R. Inhibiting islet amyloid polypeptide fibril formation by the red wine compound resveratrol. *Chembiochem*. 2009; 10:445–449. [PubMed: 19165839]

Highlights

- 21-kDa 7B2 and proSAAS blocked hIAPP fibrillation *in vitro*.
- The central region within 21-kDa 7B2 is important for the inhibition of hIAPP fibrillation.
- The N-terminal region of proSAAS is important for the inhibition of hIAPP fibrillation.
- Both chaperones blocked the cytotoxic effects of exogenous hIAPP on Rin5f cells when added exogenously.
- Overexpressed 7B2 also blocked the cytotoxic effects of exogenous hIAPP.

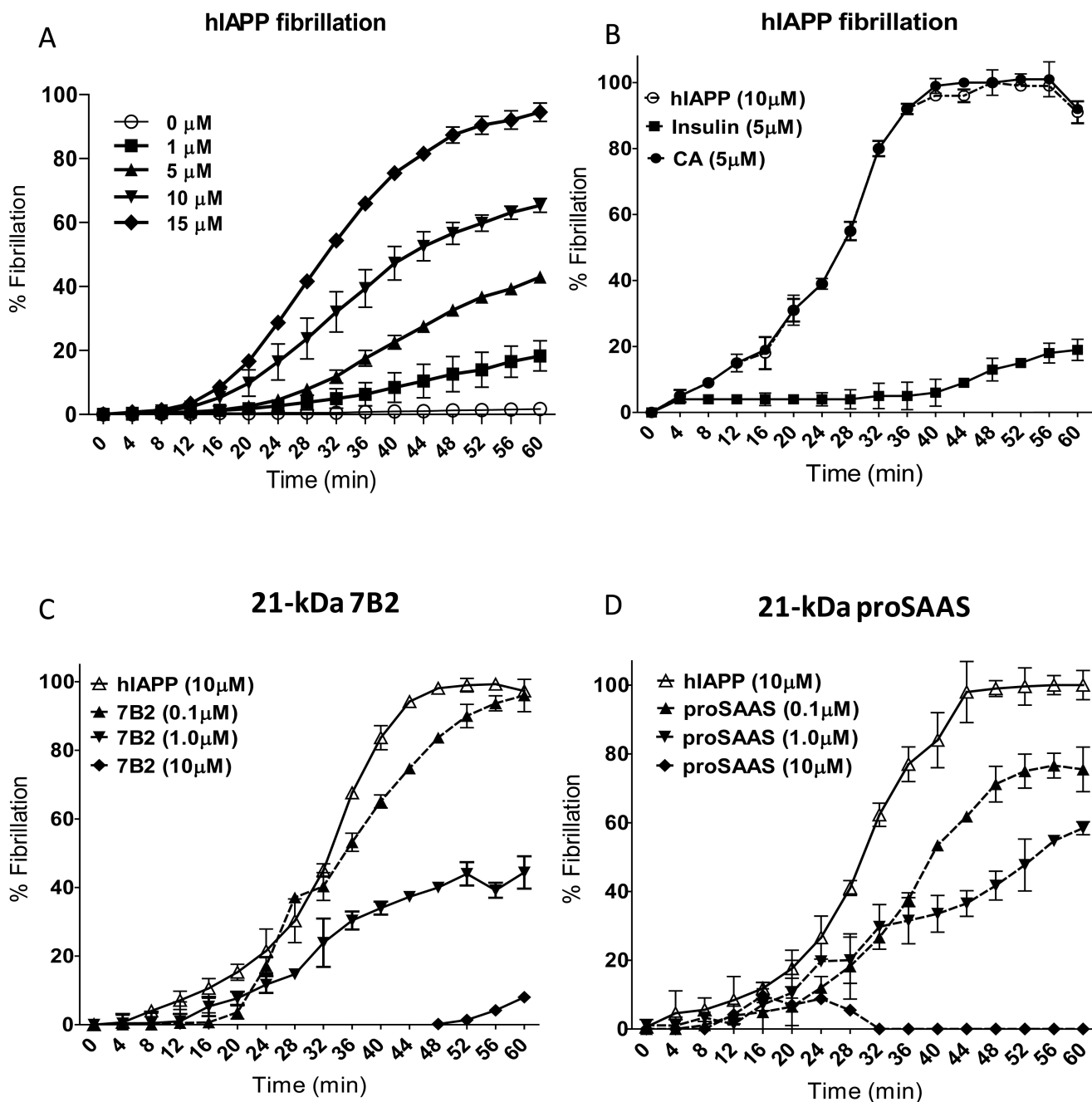


Figure 1. Dose-dependence of 21-kDa 7B2 and 21-kDa proSAAS on hIAPP fibrillation
 Changes in fibrillation kinetics according to hIAPP concentration (0 – 15 μM ; (A). hIAPP was also fibrillated in the presence of a positive (insulin) and a negative (carbonic anhydrase, CA) control (B). Dose-dependent inhibition of hIAPP by 21-kDa 7B2 (C) and 21-kDa proSAAS (D). Each fibrillation data point represents the mean \pm SD, N=3.

A



B

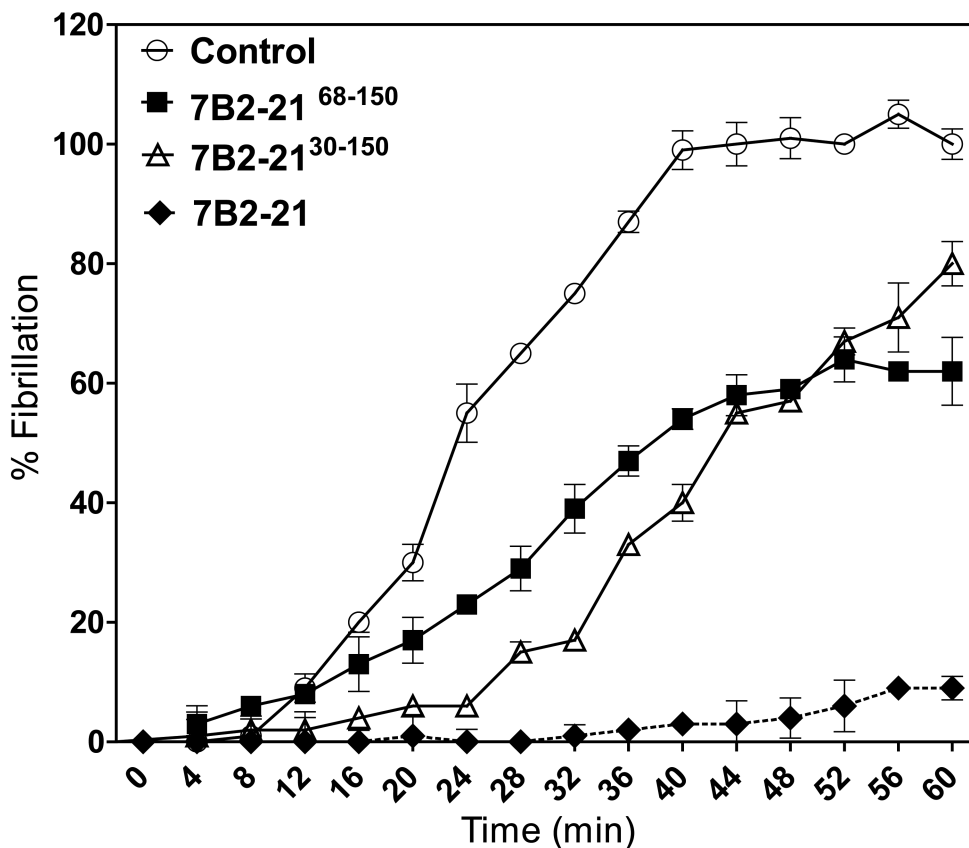
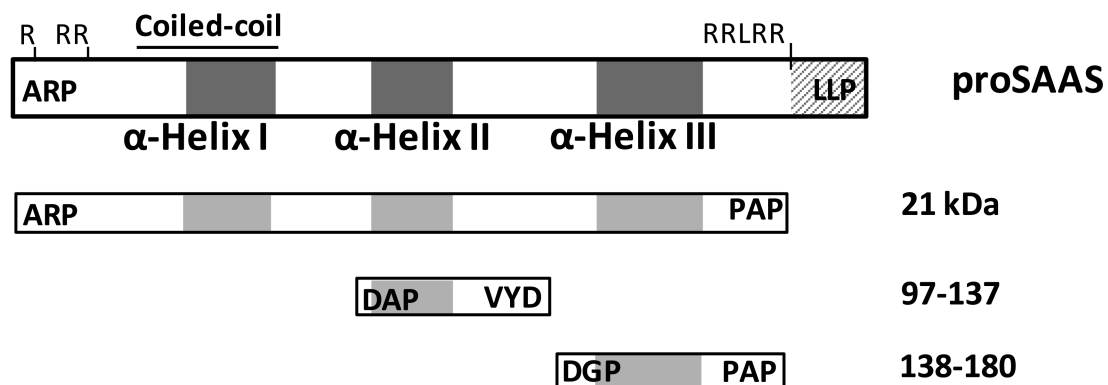


Figure 2. N-terminally truncated 7B2 proteins partially inhibit hIAPP fibrillation

Schematic diagram of 7B2 and the N-terminally truncated 7B2 constructs (A). hIAPP (10 μ M) was fibrillated in the presence of vehicle or 10 μ M of 7B2-21⁶⁸⁻¹⁵⁰ and 7B2-21³⁰⁻¹⁵⁰ constructs. The constructs block fibrillation by 40% and 20 %, respectively (B). Each fibrillation data point represents the mean \pm SD, N=3. The C-terminal peptide is indicated with a hatched square and the α -helices in gray squares.

A



B

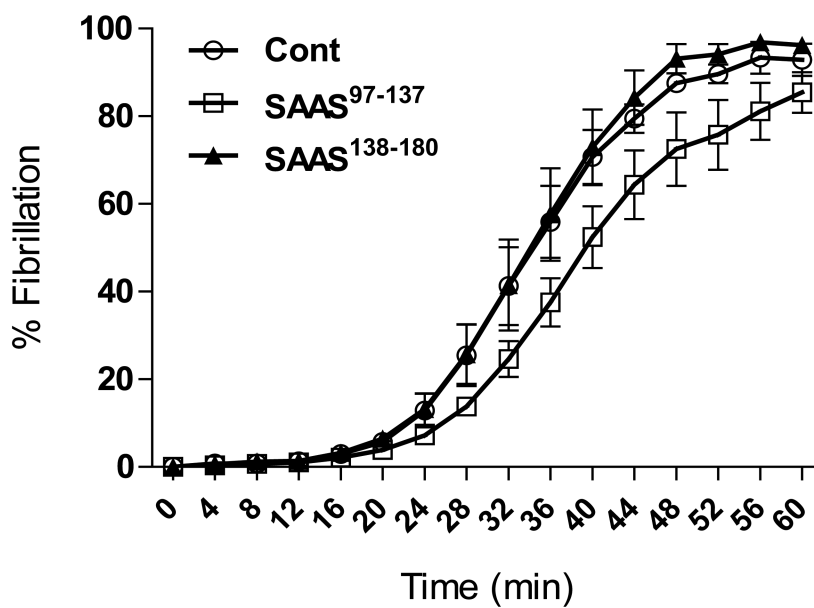


Figure 3. The α -helices II and III of proSAAS alone do not inhibit hIAPP fibrillation
 Schematic diagram of proSAAS and the proSAAS-derived peptides (A). hIAPP (10 μ M) was fibrillated in the presence of vehicle or 10 μ M of the peptides (B). Each fibrillation data point represents the mean \pm SD, N=3. The C-terminal peptide is indicated with a hatched square and the α -helices in gray squares.

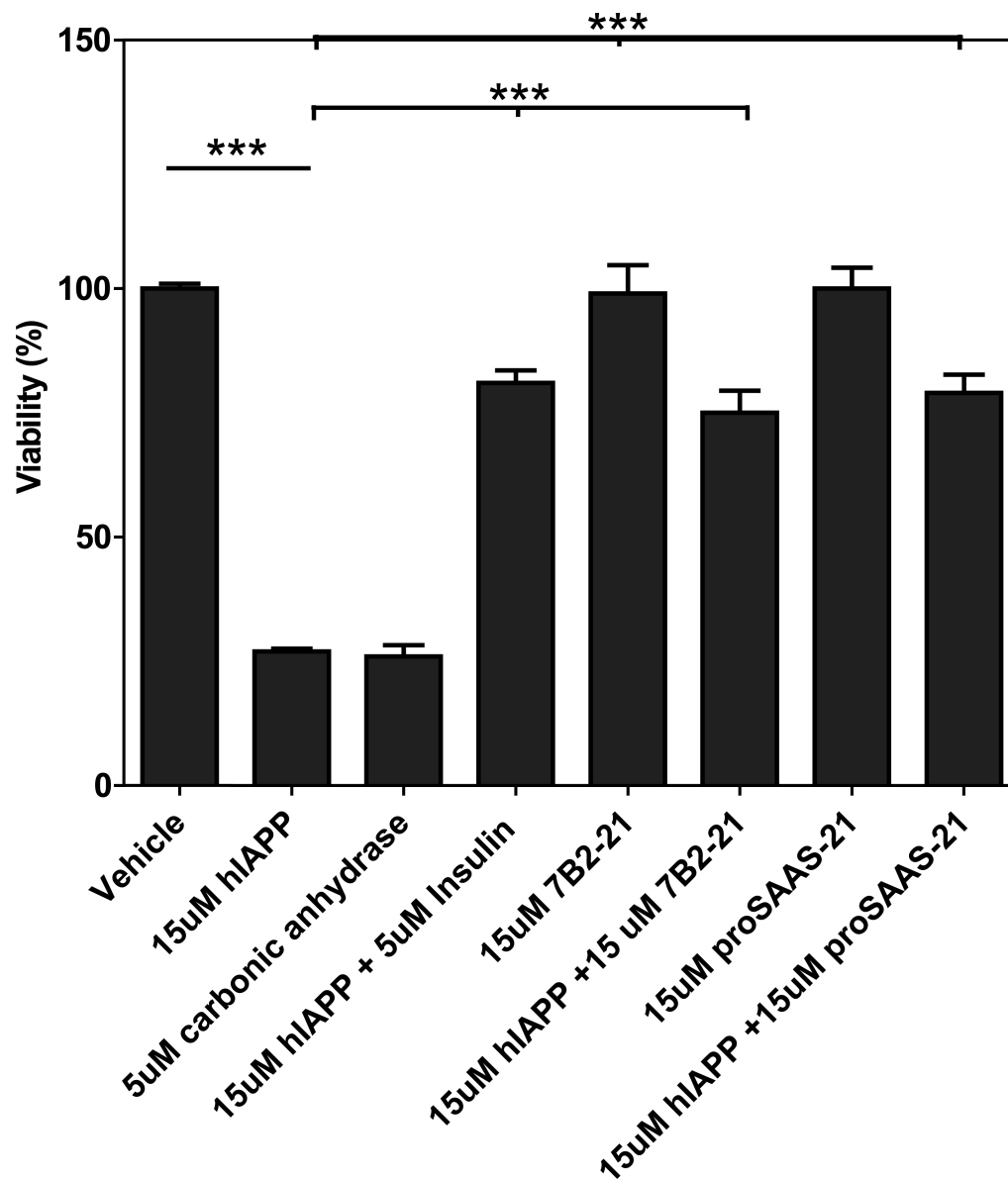


Figure 4. Both 7B2 and proSAAS block hIAPP-induced cytotoxicity in Rin5f cells
 Rin5f cells were incubated for 24 h with 15 μ M hIAPP in triplicate, resulting in 73% cytotoxicity. The inclusion of 21-kDa proSAAS and 21-kDa 7B2 (in a 1:1 molar ratio with hIAPP) to the medium during the 24 h treatment significantly blocked hIAPP-mediated cell death, as assessed by WST-1 viability assay. Carbonic anhydrase and insulin were added as negative and positive controls in an independent set of hIAPP-treated Rin5f cells. Results represent the mean \pm SD, N=3. ***, $P < 0.05$.

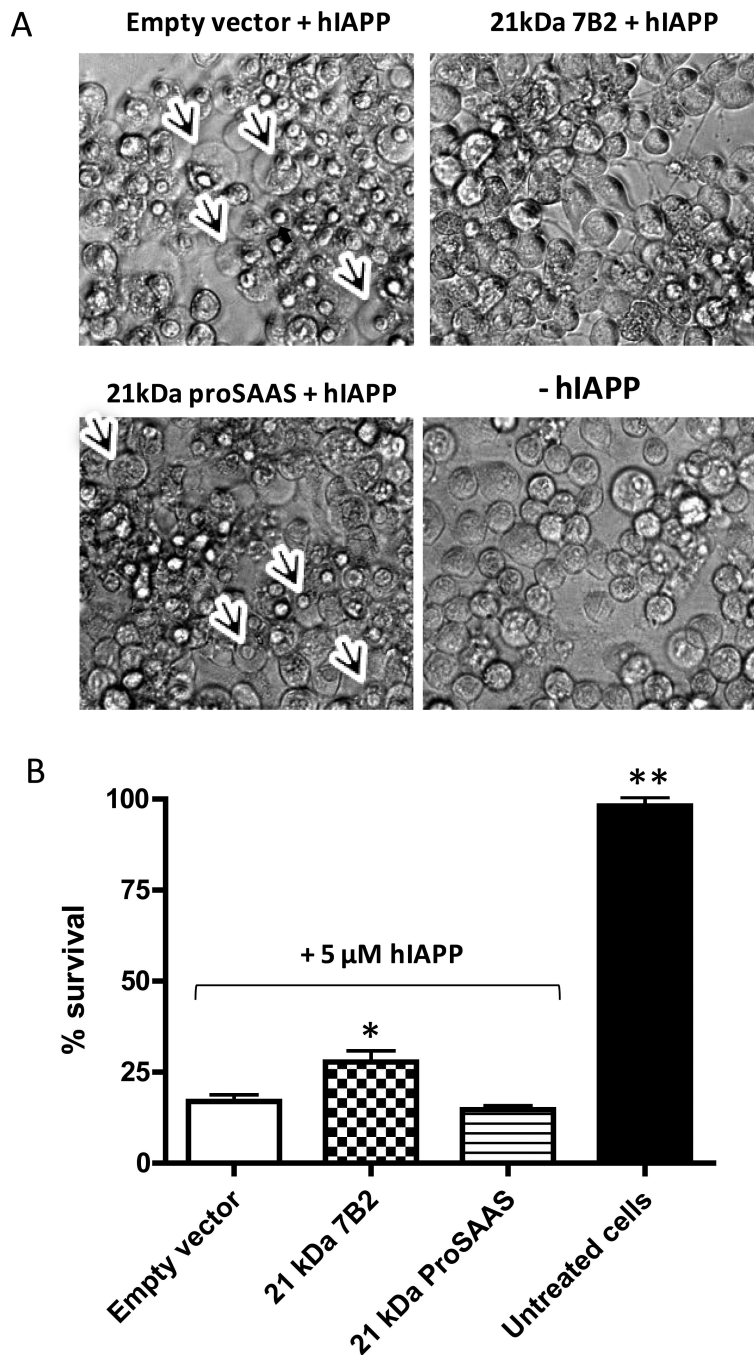


Figure 5. Transfection of 7B2 cDNA increases cell survival after hIAPP treatment in Neuro2A cells

Neuro2A cells were transfected with vectors encoding 7B2 and proSAAS (24h) and then incubated with 5 μ M hIAPP (24 h). Most of the cells transfected with the empty vector died after hIAPP treatment (A and B). Representative apoptotic cells are indicated with arrows. In contrast to proSAAS cDNA (A, bottom left) transient transfection of 21 kDa7b2 cDNA significantly increased cell survival after hIAPP treatment (B) and no apoptotic cells were observed (A, top right). * P<0.05; ** P<0.005.